J. Fluid Mech. (2009), *vol.* 633, *pp.* 137–145.
doi:10.1017/S0022112009008076 Printed in the United Kingdom

Flow separation from a stationary meniscus

J. SÉBILLEAU[1], L. LIMAT[1] AND J. EGGERS[2]†

[1]Laboratoire Matière et Systèmes Complexes, UMR CNRS 7057, Université Paris Diderot, 10 rue Alice Domon et Léonie Duquet, 75205 Paris Cedex 13, France

[2]School of Mathematics, University of Bristol, University Walk, Bristol BS8 1TW, UK

(Received 20 February 2009 and in revised form 12 May 2009)

We consider the steady flow near a free surface at intermediate to high Reynolds numbers, both experimentally and theoretically. In our experiment, an axisymmetric capillary meniscus is suspended from a cylindrical tube, held slightly above a horizontal water surface. A flow of dyed water is released through the tube into the reservoir, and flow lines are thus recorded. At low Reynolds numbers, flow lines follow the free surface, and injected water spreads horizontally inside the container. Increasing the Reynolds number, the injected fluid penetrates to a certain distance into the bath, but ultimately follows the free surface. Above a critical Reynolds number of approximately 60, the flow separates from the free surface in the meniscus region and a jet projects vertically into the bath. We find no indication that the flow reattaches at higher Reynolds numbers, nor are our findings sensitive to surface contamination. We show theoretically and confirm experimentally that the separating streamline forms a right angle with the free surface.

1. Introduction

If one solves for inviscid irrotational flow with either solid or free surfaces, streamlines remain attached to the surface. However, these solutions do not obey the correct boundary conditions for viscous flow at the surface, even if the viscosity is small. As a result, in the limit of small viscosity, a thin boundary layer forms. In the case of a solid body, this is one of the most widely studied problems in fluid mechanics. It is well known that at high Reynolds numbers the boundary layer will detach from the body, and streamlines that followed the surface enter the flow (Schlichting 1987; Smith 1986; Sychev *et al.* 1998). This fact has profound consequences for the nature of the flow, like the lift and the viscous drag on the body, the stability of the flow and the generation of vorticity.

By comparison, very little is known about separation from a free surface, and there is little accepted theory beyond the discussion found in the classical textbook by Batchelor (1967), but see Leal (1989) for a progress report. Based on the description of unseparated free-surface boundary layer flow (Moore 1963; Harper & Moore 1968; Harper 1972), the main conclusion is that separation is much less likely to occur from free boundaries than from solid ones. In particular, in the limit of high Reynolds numbers the flow is predicted to always remain attached to the free surface. This statement has been confirmed by numerical simulations of flow around 'bubbles' of fixed ellipsoidal shape (Dandy & Leal 1986; Blanco & Magnaudet 1995). It is found that first a separation bubble forms at a lower critical Reynolds number Re_1, but the

† Email address for correspondence: jens.eggers@bris.ac.uk

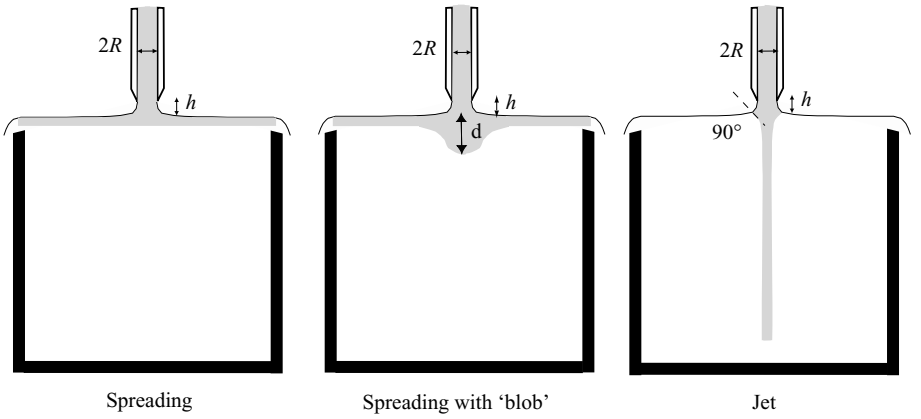

FIGURE 1. Schematic of the experimental set-up and the different regimes observed.

flow later reattaches at a second, higher critical Reynolds number Re_2. The upper value Re_2, in particular, increases rapidly with the aspect ratio χ of the ellipsoidal bubble.

In spite of these theoretical results, it is clear that, in practice, separation from a free surface is very prevalent over a wide range and including very high Reynolds numbers. For example, 'scars' that are formed on a free surface (Brocchini & Peregrine 2001*a*,*b*) point to the existence of streamlines leaving the free surface. Other indirect evidence is provided by the air that is entrained into the fluid, even at high Reynolds number (Lin & Donnelly 1966; Bin 1993). Another example is the instability of gas bubbles rising in water, for which the existence of a separated wake behind the bubble is a prerequisite (Magnaudet & Mougin 2007; Zenit & Magnaudet 2008). As pointed out by Zenit & Magnaudet (2008), one important reason why the flow stays separated at high flow speeds is that the free surface deforms so as to promote separation. For example, a rising bubble becomes increasingly flat at higher rise speeds, so that the Reynolds number remains well below the critical value Re_2 for the flat bubble, which has a large χ.

In this paper, we use the steady flow through a capillary meniscus to investigate flow separation from a free surface. This permits to study the flow geometry near a free surface over a wide range of Reynolds numbers. Meanwhile, the shape of the meniscus remains relatively undisturbed, so we are in a position to look at the transition from unseparated to separated flow, just using the Reynolds number as a single parameter. We are not aware of any previous experimental study that has looked at this transition, or at the flow geometry close to the point of separation. In the following section, we introduce the meniscus flow experiment, and describe the transition to separated flow as the flow rate is increased. We show that the flow geometry is controlled by the Reynolds number alone. In the next section we show theoretically that the flow at separation is a stagnation point flow. This is confirmed experimentally by showing that flow lines leave the free surface at a right angle. In the case of solid boundaries, by contrast, separation occurs tangentially in the limit of large Re (Smith 1986).

2. Meniscus flow experiment

A schematic of the experimental set-up is shown in figure 1. Water is injected from a flexible tube of radius R into a glass box (10 cm × 10 cm × 10 cm) filled with

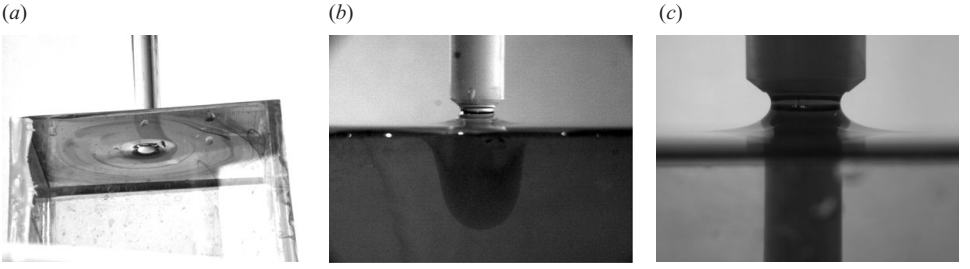

FIGURE 2. Photographs of the experiment, for flow rates $Q = 0.06$ cm^3 s^{-1}, 0.27 cm^3 s^{-1} and 2.46 cm^3 s^{-1}, which correspond to $Re = 4.8$, 21.5 and 198. The Weber numbers are $We = 8 \times 10^{-4}$, 1.6×10^{-3} and 0.14. (*a*) The free surface is shown from below to show the horizontal spreading. For the intermediate flow rate, a blob of depth $d = 1.6$ cm is formed, but the flow ultimately spreads. (*c*) the flow detaches from the highly curved meniscus at a right angle to form a jet.

water. A capillary meniscus is produced by first dipping the tube into the water, and then withdrawing it carefully. Normally this is done to produce the greatest possible elevation of the tube h for which the meniscus is still stable. However, we also performed some experiments with smaller values of h.

The fluid is injected at a constant rate, and is allowed to overflow, ensuring a stationary situation. The flow is driven by the constant pressure head between the container and a reservoir, which is fed by a pump and is overflowing as well. This guarantees a constant flow rate and minimal perturbations to the flow. For each experiment, we allowed for several minutes for the flow to reach a stationary state. We then injected carefully a small amount of ink into the tube close to its opening. Great care was taken for the ink to have the same density as the water; the difference is less than two parts in 1000. As the coloured water spreads, a sharp boundary between the moving fluid coming from the pipe (dark) and the almost quiescent fluid in the container (light) becomes visible (figure 2).

At low flow rate Q, the coloured water spreads along the surface, remaining confined to a thin surface layer (figure 2*a*). At moderate flow rate, the coloured water still spreads on the surface, but the flow penetrates the stagnant water under the injection tube, leading to formation of a 'blob' (figure 2*b*). At high flow rate, the coloured region is confined to a jet penetrating the stagnant water, while the horizontal surface remains clear. A streamline that was once following the free surface leaves the free surface at a stagnation point and subsequently marks the boundary of the jet (figure 2*c*).

As we will see below, the most significant dimensionless control parameter responsible for the appearance of the flow is the Reynolds number $Re \equiv RU/\nu = Q/(\pi\nu R)$, where ν is the kinematic viscosity of the fluid ($\nu = 1\,\mathrm{mm^2\,s^{-1}}$ for water). Another dimensionless control parameter is the Weber number $We = \rho RU^2/\gamma = \rho Q^2/(\pi^2 R^3 \gamma)$, where γ is the surface tension and ρ the density. Even for the highest flow rate shown in figure 2, *We* is only 0.14, indicating that inertial forces are small compared to surface tension, and the free surface shape should thus be close to that of a *static* capillary meniscus. The geometrical parameter h/R based on the elevation h is also found to be of little significance, see below.

To investigate the transition between the spreading regime and the jet regime more quantitatively, we measure the maximum depth d of the blob as function of flow rate for three different tube radii, as shown in figure 3(*a*). It is observed that d increases sharply with increasing flow rate. For each radius, the largest d corresponds

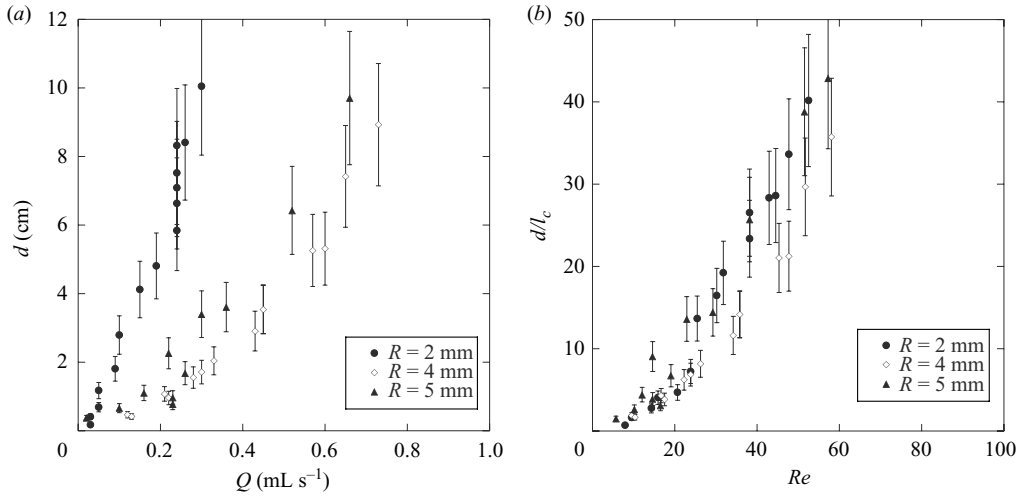

FIGURE 3. The depth of the 'blob' as function of flow rate for different radii of the injection tube. (*a*) The raw data for three different tube radii. The error bars are based on several realizations of the same experiment; the reproducibility of the experiment is usually to within 20 %. (*b*) Same data are plotted as function of Reynolds number, and are seen to collapse to within the error.

to the highest flow rate for which an attached flow was possible. For higher flow rates (whose value depends on R), the flow was always separated. The same data are presented in figure 3(*b*), but as function of the Reynolds number; the depth d is made dimensionless with the capillary length $\ell_c = \sqrt{\gamma/(\rho g)}$. The latter is a relevant length scale for the blob since it measures the curvature of the meniscus, and thus the curvature of streamlines as they pass from the tube to horizontal spreading. It is found that within the experimental uncertainty all data collapse onto a single curve, confirming the Reynolds number as the relevant control parameter.

The collapsed data set contains no point corresponding to attached flow above $Re = 60$ (figure 3*b*). Moreover, the data are consistent with a second-order transition, that is, with a diverging d as a critical Reynolds number $Re_c \approx 60$ is approached. This would correspond to a smooth transition of, say, $1/d$ towards its vanishing value as the jet is established. However, there is too much scatter as to be sure about this, and the true curve may well extrapolate to a finite value of d at $Re = 60$, corresponding to a discontinuous or first-order transition.

A possible interpretation of this latter scenario would be that there exists a flow solution which remains attached above $Re = 60$. However, this solution might become unstable at some finite Reynolds number (60 in our case), owing to small perturbations such as surface impurities or perturbations from the inlet. We also considered possible reattachment of flow lines at even higher Reynolds numbers, which is expected on theoretical grounds (Batchelor 1967, p. 364), in the case of a fixed free surface shape. However, we found no evidence for reattachment for Reynolds numbers up to 5500, which is the highest our set-up allows. Thus, at least for a real air–water interface, the theoretical argument seems to be of little practical significance. Whatever be the case, note that a typical Reynolds number for jet formation is far lower in the case of separation from a solid boundary. For example, if fluid is injected through an orifice in a solid wall, a jet is formed above $Re \approx 5$, depending on the sharpness of the orifice's corner (Birkhoff & Zarantonello 1957, p. 274).

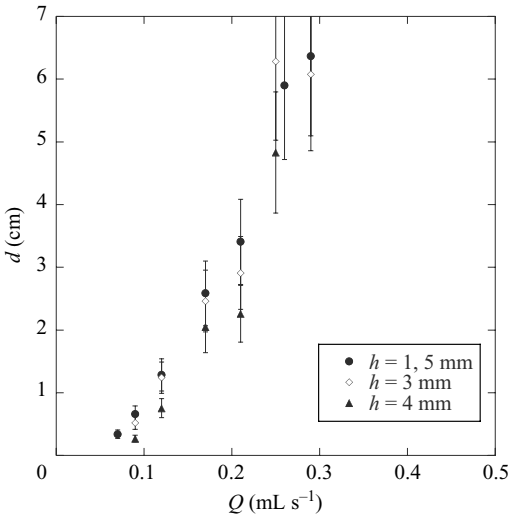

FIGURE 4. The depth of the 'blob' as function of flow rate for different meniscus heights.

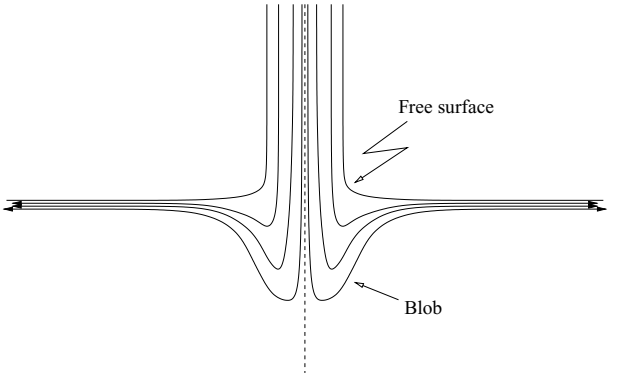

FIGURE 5. A sketch of the likely geometry of the flow in the case of a blob.

Another issue we considered was the characteristic length scale that determines the penetration depth d. All the results shown previously have been obtained with the biggest obtainable height of meniscus ($h \sim 5$ mm). To study the influence of this height, we have performed experiments with different meniscus sizes, using the narrowest tube $R = 2$ mm. As seen in figure 4, we cannot detect a significant influence on the depth of the blob. As shown in the previous figure 3, the same is true for the tube radius as well, leaving ℓ_c as the most likely parameter. Of course, the capillary length is a difficult parameter to vary, so we do not possess positive confirmation that the data will collapse when plotting d/ℓ_c.

In closing this section, we present a cartoon of how flow lines are likely to look in the case of a blob, for which separation has not yet occurred, cf. figure 5. As a result, one flowline must follow the free surface, drawn as a bold line. On the other hand, a flow line just off the centre must be close to the stagnation at the bottom of the blob, and must subsequently trace the lower boundary of the blob. All flow lines will eventually end up in a thin layer close to the free surface. It would of course be desirable to measure the flow lines in the interior of the flow directly, but this is

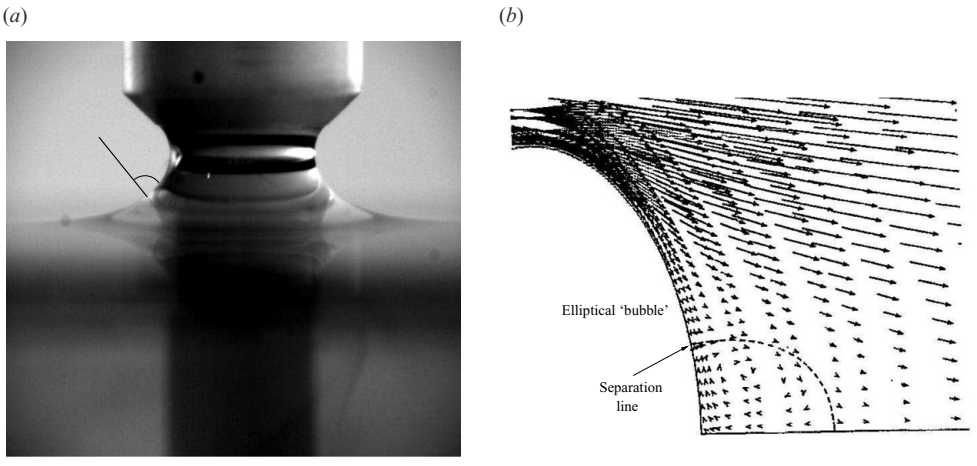

FIGURE 6. Examples of the flow near separation from a free surface. (*a*) A closeup of the meniscus region, taken from one of our experiments. The parameters are $Q = 1.6$ cm^3 s^{-1}, $Re = 127$ and $We = 0.056$, for which we observe separated flow. (*b*) One quadrant of a numerical simulation of the two-dimensional flow around an elliptical obstacle ('bubble') with free slip boundary condition (Blanco & Magnaudet 1995). The aspect ratio of the ellipse is $\chi = 1.75$, and $Re = 100$, based on the major axis. In both cases, the flow is seen to separate at a right angle.

not easy without perturbing the free surface substantially be the presence of tracer particles.

3. Analysis of separation

We now focus on the neighbourhood of the point of separation, as seen in the two examples of figure 6. The flow separates from the free surface in the highly curved meniscus region at a right angle, as first shown by Lugt (1987). This fact is a simple consequence of the boundary condition at the free surface, which is stress free. We also assume that the flow is stationary, so the normal velocity at the surface vanishes as well. In general, a potential flow will not obey the free stress condition, so the derivation relies on the fluid being viscous, although the flow equations themselves are not required.

In the following, for simplicity we are going to restrict ourselves to two-dimensional flow. This does not represent any loss of generality, since the third dimension can be taken in the direction of the line of separation. As shown in figure 7, we approximate the free surface to second order by an inscribed circle of radius R, where $\kappa = R^{-1}$ is the curvature of the intersection of the free surface with the plane of the flow. Using polar coordinates (r, ϕ), the free surface is given locally by the coordinate line $r = R$. Then from the free-surface boundary condition the vanishing component of the stress tensor $\boldsymbol{\sigma}$ is given by

$$\boldsymbol{\sigma}_{r\phi} = \nu\rho \left[\kappa \frac{\partial u_r}{\partial \phi} + \frac{\partial u_\phi}{\partial r} - \kappa u_\phi \right] = 0, \tag{3.1}$$

and the (two-dimensional) vorticity is

$$\omega = \kappa \frac{\partial u_r}{\partial \phi} - \frac{\partial u_\phi}{\partial r} - \kappa u_\phi, \tag{3.2}$$

where we have used $r \approx R$.

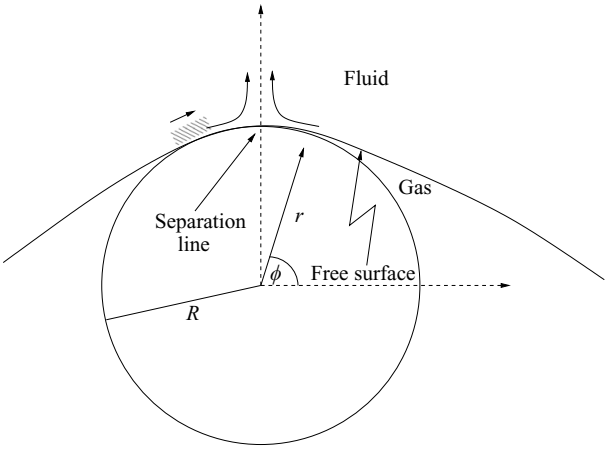

FIGURE 7. The local coordinate system and geometry of a flow near a point of separation from a free surface.

Since the interface is stationary, we have $u_r = 0$ for $r = R$ and thus $\partial u_r/\partial\phi = 0$ near the surface. Combining (3.1) and (3.2), we obtain the well-known relationship (Batchelor 1967):

$$\omega = -2\kappa u_\phi, \tag{3.3}$$

between the vorticity on the surface and the curvature of the interface. The physical interpretation of (3.3) is clarified by expanding the local velocity field near the surface:

$$\delta u_{r/\phi} = \frac{\partial u_{r/\phi}}{\partial r}\delta r + \frac{\partial u_{r/\phi}}{\partial \phi}\delta\phi. \tag{3.4}$$

Using (3.1) and (3.3), we have

$$\frac{\partial u_\phi}{\partial r} = \kappa u_\phi = -\frac{\omega}{2}. \tag{3.5}$$

With this relation as well as incompressibility, (3.4) can be simplified to

$$\delta u_r = k\delta r, \quad \delta u_\phi = -kR\delta\phi - \frac{\omega}{2}\delta r, \tag{3.6}$$

where $k = \partial u_r/\partial r$ is the local strain rate.

Equation (3.6) implies that the flow near the free surface (shaded region in figure 7) is a superposition of a straining flow and a free body rotation. The reason is that a fluid element is free of shear stress, so up to a straining motion the fluid element is in solid body rotation (cf. Longuet-Higgins 1992). But at the stagnation point $u_\phi = 0$, so ω vanishes as well according to (3.3). This means that (3.6) simplifies to an irrotational stagnation point flow (cf. figure 7), which in a Cartesian coordinate system centred at the point of separation is

$$u = -kx, \quad v = ky. \tag{3.7}$$

Here x is reckoned in the tangential flow direction, and is y normal to it. Equation (3.7) also implies that the separating streamline leaves the free surface at a right angle. This is geometrically obvious, since the local speed of rotation changes sign at the stagnation point. The only possible exception is the degenerate case $k = 0$, which is discussed further in Lugt (1987), but is irrelevant here because it would involve more than one separating streamline.

4. Discussion

We have presented a simple, steady flow experiment which documents the transition from unseparated to separated flow. The two flows are radically different, in that the latter permits (coloured) water from the tube to enter the reservoir, while with the former flow, the fluid in the reservoir remains virtually undisturbed. However, the transition is gradual to a certain degree, in that close to a critical Reynolds number the penetration depth d becomes large. It is difficult to be certain about the order of the transition, i.e. whether d actually diverges at Re_c, but this question deserves further attention. To assess the role of a possible contamination of the water surface, we have also performed preliminary experiments with 0.2 % weight of the surfactant SDS (sodium dodecyl sulphate) added to the water. SDS has a significant surface activity, and reduces the surface tension to about half the value of pure water at this concentration. However, within the scatter of our data, there is no change in the critical flow rate at which transition to jetting occurs. This indicates that the purity of the water surface is not critical for our experimental results. However, it might still be worthwhile to perform more experiments with a non-polar fluid, which guarantees a much cleaner interface (Zenit & Magnaudet 2008).

It has been proposed by Leal (1989) that a local condition for the appearance of separation is that the surface vorticity has reached a certain critical value. According to (3.5) it would be enough (apart from recording the free surface shape) to measure the surface velocity in order to test this hypothesis. However, since we show that at separation the surface vorticity is actually zero, the criterion is not straightforward to apply. In view of the simplicity of the geometry, numerical simulations would also be well feasible. A slight conceptual problem associated with the present experiment is that a certain amount of vorticity is generated in the tube which feeds the flow. However, the maximum vorticity in the tube scales like U/R, and we have checked that for all values of Re considered, the flow is a fully developed Poiseuille flow at the tube outlet. The fact that our data collapse as function of $Re = UR/\nu$ is thus an indication that this vorticity injection does not play a major role. Numerical simulations would also be of great value in examining the issue of reattachment at high Reynolds numbers, since non-deformable, ideally free interfaces can be implemented theoretically but are difficult to approximate experimentally.

We owe the inspiration for this work to our late colleague Howell Peregrine. We are grateful to Maurice Rossi for helpful conversations and for pointing out Lugt's work to us.

REFERENCES

Batchelor, G. K. 1967 *An Introduction to Fluid Dynamics*. Cambridge University Press.

Bin, A. K. 1993 Gas entrainment by plunging liquid jets. *Chem. Engng Sci.* **48**, 3585–3630.

Birkhoff, G. & Zarantonello, E. H. 1957 *Jets, Wakes, and Cavities*. Academic.

Blanco, A. & Magnaudet, J. 1995 The structure of the axisymmetric high-Reynolds-number flow around an ellipsoidal bubble of fixed shape. *Phys. Fluids* **7**, 1265–1274.

Brocchini, M. & Peregrine, D. H. 2001*a* The dynamics of strong turbulence at free surfaces. Part 1. Description. *J. Fluid Mech.* **449**, 225–254.

Brocchini, M. & Peregrine, D. H. 2001*b* The dynamics of strong turbulence at free surfaces. Part 2. The boundary conditions. *J. Fluid Mech.* **449**, 255–290.

Dandy, D. S. & Leal, L. G. 1986 Boundary-layer separation from a smooth slip surface. *Phys. Fluids* **29**, 1360–1366.

Harper, J. F. 1972 Motion of bubbles and drops through liquids. *Adv. Appl. Mech.* **12**, 59–129.

Harper, J. F. & Moore, D. W. 1968 The motion of a spherical liquid drop at high Reynolds number. *J. Fluid Mech.* **32**, 367–391.

Leal, L. G. 1989 Vorticity transport and wake structure for bluff bodies at finite Reynolds number. *Phys. Fluids* A **1**, 124–131.

Lin, T. J. & Donnelly, H. G. 1966 Gas bubble entrainment by plunging laminar liquid jets. *AIChE J.* **12**, 563–571.

Longuet-Higgins, M. S. 1992 Capillary rollers and bores. *J. Fluid Mech.* **240**, 659–679.

Lugt, H. J. 1987 Local flow properties at a viscous free surface. *Phys. Fluids* **30**, 3647–3652.

Magnaudet, J. & Mougin, G. 2007 Wake instability of a fixed spheroidal bubble. *J. Fluid Mech.* **572**, 311–337.

Moore, D. W. 1963 The boundary layer on a spherical gas bubble. *J. Fluid Mech.* **16**, 161–176.

Schlichting, H. 1987 *Boundary Layer Theory*, 7th edn. McGraw-Hill.

Smith, F. T. 1986 Steady and unsteady boundary layer separation. *Ann. Rev. Fluid Mech.* **18**, 197–220.

Sychev, V. V., Ruban, A. I., Sychev, V. V. & Korolev, G. L. 1998 *Aymptotic Theory of Separated Flows*. Cambridge University Press.

Zenit, R. & Magnaudet, J. 2008 Path instability of rising spheroidal bubbles: a shape-controlled process. *Phys. Fluids* **20**, 061702 (1–4).